The 2010 IEEE/RSJ International Conference on
Intelligent Robots and Systems
October 18-22, 2010, Taipei, Taiwan

Iterative Learning Control for a Redundant Musculoskeletal Arm: Acquisition of Adequate Internal Force

Kenji Tahara and Hitoshi Kino

Abstract— **This paper presents a proposal of an iterative learning control method for a musculoskeletal arm to acquire adequate internal force to realize human-like natural movements. Additionally, a dynamic damping ellipsoid at the end-point is introduced to evaluate internal forces obtained through the iterative learning. In our previous works, we have presented that a human-like smooth reaching movement using a musculoskeletal redundant arm model can be obtained by introducing a nonlinear muscle model and "the Virtual spring-damper hypothesis". However, the internal forces have been determined heuristically, so far. In this paper, an iterative learning control method is used for acquisition of an adequate dynamic damping ellipsoid according to a given task, in order to determine internal forces more systematically. It is presented that the learning control scheme can perform effectively to realize given desired tasks, even under the existence of strong nonlinear characteristics of the muscles. After acquiring a given task, the dynamic damping ellipsoid is introduced to evaluate the relation between a damping effect generated by the acquired internal forces and a trajectory of the end-point. Some numerical simulations are performed and the usefulness of the learning control strategy, despite strong nonlinearity of the muscles, is demonstrated through these results.**

I. INTRODUCTION

Humans' movements are much more smooth, dexterous, and natural than those of present robots. Up to now, many robotics researchers have devoted attention to the acquisition of such human-like movements; it remains a hot topic in robotics. However, several difficulties remain in realizing such human-like movements. To surmount such difficulties, we should specifically examine the existence of redundancy of two types, which a human body intrinsically possesses. One is joint redundancy, whereby the number of joints is greater than the dimensions of the task space. The other is muscle redundancy, by which several muscles are related to the actuation of one joint. Both redundancies might enhance dexterity and versatility of human movements. However, they each induce different ill-posed problems [1]. Joint redundancy causes an ill-posed problem that each joint angle cannot be determined uniquely corresponding to a given end-point position of the arm. Muscle redundancy raises another problem: the set of muscular forces to realize a given desired joint torque cannot be determined uniquely. Many optimization methods to overcome these ill-posed problems arising from such redundancies have been proposed in the fields of physiology and robotics to date [2–4]. In recent years, Arimoto *et al*. [5] proposed a novel hypothesis, called "the Virtual spring-damper hypothesis": no optimization criteria are necessary to overcome the ill-posed problem related to joint redundancy. Expanding the virtual spring-damper hypothesis, we have treated the other problem caused by muscle redundancy in our previous study [6]. Based on the result, we proposed an index by introducing a nonlinear muscle model to determine the internal force generated by redundant muscles. This nonlinear muscle model enables modulation of the joint damping effect by changing the internal forces generated by redundant muscles. Therefore, this feature can give internal forces physical meaning to determine it uniquely. However, in our previous studies, an adequate value of the internal force has been chosen heuristically to realize a human-like natural movement. The main objective of the paper is to discuss how to determine an adequate internal force to realize human-like natural movements when a desired trajectory is given initially [7]. To do this, first an iterative learning control scheme [8] is proposed to realize a given desired end-point trajectory. Previous studies related to iterative learning control did not treat any kind of muscle dynamics which includes strong nonlinearity. Unlike those earlier studies, this paper demonstrates for the first time that the iterative learning control method is applicable to obtain a suitable damping effect, even given the existence of strong nonlinearity of the muscle dynamics. Secondly, the dynamic damping ellipsoid at the end-point of the arm is introduced to evaluate the damping effect. Some numerical simulations are conducted. These results demonstrate that the iterative learning control scheme can realize a desired trajectory even though our muscle model includes strong nonlinearity. Through evaluation of the acquired internal force pattern using the dynamic damping ellipsoid, we discuss how to determine an adequate internal force uniquely to realize human-like natural movements.

II. MUSCULO-SKELETAL ARM MODEL

A redundancy-driven musculoskeletal arm comprising two links, four monoarticular muscles, and two biarticular muscles is modeled in this paper. In our previous work [6], both joint and muscle redundancies were examined, but this paper treats only muscle redundancy because of focusing on the internal forces generated by redundant muscles. The model presented herein is shown in Fig. 1. Assume that the overall

This work was partially supported by Japan Society for the Promotion of Science (JSPS), Grant-in-Aid for Scientific Research (C) (20560249), and "the Kyushu University Research Superstar Program (SSP)", based on the budget of Kyushu University allocated under President's initiative.

K. Tahara is with the Institute for Advanced Study, Kyushu University, 744 Moto'oka, Nishi-ku, Fukuoka 819-0395, Japan tahara@ieee.org

H. Kino is with the Department of Intelligent Mechanical Engineering, Fukuoka Institute of Technology, 3-30-1 Wajiro-higashi, Higashi-ku, Fukuoka 811-0295, Japan kino@fit.ac.jp

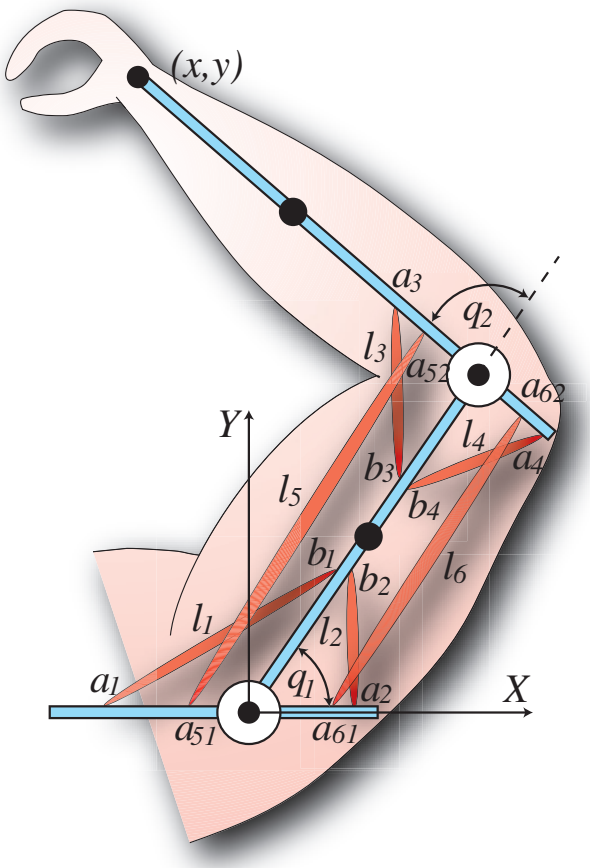

Fig. 1. Two-link planar arm model with six muscles.

movements are restricted in a horizontal plane, the gravity effect can be ignored in this model. Each skeletal muscle is approximated as a linear segment so that its contraction is linear, and its mass transfer during contraction is omitted for simplicity.

A. Kinematics

Suppose that a muscle length vector $\boldsymbol{l} = [l_1, l_2, \cdots, l_6]^{\mathrm{T}} \in \mathbb{R}^6$ can be expressed by a joint angle vector $\boldsymbol{q} = [q_1, q_2]^{\mathrm{T}} \in \mathbb{R}^2$ in the following way:

$$\boldsymbol{l} = \boldsymbol{G}_l(\boldsymbol{q}) \in \mathbb{R}^6, \tag{1}$$

where $\boldsymbol{G}_l(\boldsymbol{q})$ in the right-hand side of (1) is a nonlinear vector that expresses the relation between each joint angle and each muscle length. Namely, it indicates the forward kinematics from the joint angle space to the muscle length space. Moreover, the time derivertive of (1) is given in the following:

$$\dot{\boldsymbol{l}} = \boldsymbol{W}^{\mathrm{T}}\dot{\boldsymbol{q}} \in \mathbb{R}^6, \tag{2}$$

where $\boldsymbol{W}^{\mathrm{T}} \in \mathbb{R}^{6\times 2}$ is the Jacobian matrix for each muscle contractile velocity with respect to each joint angular velocity, and hereafter, it is called "the muscle Jacobian matrix". On the other hand, the relation between each muscular force $\boldsymbol{f}_m \in \mathbb{R}^6$ and each joint torque $\boldsymbol{\tau} \in \mathbb{R}^2$ can be given through the principle of virtual work in the following manner:

$$\boldsymbol{\tau} = \boldsymbol{W}\boldsymbol{f}_m \in \mathbb{R}^2, \tag{3}$$

where we assume that the muscle Jacobian matrix $\boldsymbol{W} \in \mathbb{R}^{2\times 6}$ is of row full-rank during movement. The inverse relation of (3) can be given in the following way:

$$\boldsymbol{f}_m = \boldsymbol{W}^{+}\boldsymbol{\tau} + \left(\boldsymbol{I}_6 - \boldsymbol{W}^{+}\boldsymbol{W}\right)\boldsymbol{k} \in \mathbb{R}^6, \tag{4}$$

where $\boldsymbol{W}^{+} = \boldsymbol{W}^{\mathrm{T}}(\boldsymbol{W}\boldsymbol{W}^{\mathrm{T}})^{-1} \in \mathbb{R}^{6\times 2}$ stands for the pseudo-inverse matrix of $\boldsymbol{W}$ and $\left(\boldsymbol{I}_6 - \boldsymbol{W}^{+}\boldsymbol{W}\right)\boldsymbol{k} \in \mathbb{R}^6$ implies the null-space of $\boldsymbol{W}$. and $\boldsymbol{k} \in \mathbb{R}^6$ is an arbitrary vector. The physical meaning of the null-space is that space in which internal forces are generated by the configuration of redundant muscles. In addition, the relation between the joint torque $\boldsymbol{\tau}$ and the output forces of the end-point in the inertia frame $\boldsymbol{F} \in \mathbb{R}^2$ is given as

$$\boldsymbol{\tau} = \boldsymbol{J}^{\mathrm{T}}\boldsymbol{F} \in \mathbb{R}^2. \tag{5}$$

where $\boldsymbol{J} \in \mathbb{R}^{2\times 2}$ denotes the Jacobian matrix for the end-point velocity with respect to each joint angular velocity. Substituting (5) into (4) yields:

$$\boldsymbol{f}_m = \boldsymbol{W}^{+}\boldsymbol{J}^{\mathrm{T}}\boldsymbol{F} + \left(\boldsymbol{I}_6 - \boldsymbol{W}^{+}\boldsymbol{W}\right)\boldsymbol{k} \in \mathbb{R}^6. \tag{6}$$

Equation (6) shows the relation between the muscular force and the output force of the end-point.

On the other hand, the end-point position vector $\boldsymbol{x} \in \mathbb{R}^2$ in the task space can be expressed by the joint angle vector $\boldsymbol{q} \in \mathbb{R}^2$ as

$$\boldsymbol{x} = \boldsymbol{G}_x(\boldsymbol{q}) \in \mathbb{R}^2, \tag{7}$$

where $\boldsymbol{G}_x(\boldsymbol{q})$ is a nonlinear vector that expresses the relation between each joint angle and an end-point position. Namely, it denotes the forward kinematics from the joint angle space to the end-point position space.

The time derivertive of (7) is also given as follows:

$$\dot{\boldsymbol{x}} = \boldsymbol{J}\dot{\boldsymbol{q}} \in \mathbb{R}^2. \tag{8}$$

As mentioned previously, we consider a non-joint-redundant two link planar arm model in this paper, and assume that an attitude of the arm does not become singular during movement. Therefore, we can easily obtain the inverse relation of (7) and (8) in the following way:

$$\boldsymbol{q} = \boldsymbol{G}_x^{-1}(\boldsymbol{x}) \in \mathbb{R}^2 \tag{9}$$

$$\dot{\boldsymbol{q}} = \boldsymbol{J}^{-1}\dot{\boldsymbol{x}} \in \mathbb{R}^2, \tag{10}$$

where $\boldsymbol{G}_x^{-1}(\boldsymbol{x})$ in the right-hand side of (9) signifies a nonlinear vector which indicates the inverse kinematics from the end-point position space to the joint angle space. Also, (10) denotes the differential inverse kinematics from the end-point velocity space to the joint angular velocity space.

B. Nonlinear Muscle Model

In this paper, we introduce the nonlinear muscle model which has already been proposed in our previous work [6]. In physiology, Hill's muscle model, in which the force–velocity relation of the skeletal muscle is expressed as a simple hyperbolic equation, is formulated as

$$(f_m + a)(\dot{l} + b) = b(f_0 + a), \tag{11}$$

where f_m signifies the output contractile force, $\dot{l}$ is the contralctile velocity, f_0 denotes the maximum isometric contractile force, whose magnitude depends on its own length. Furthermore, a and b are the heat constant and the rate constant with respect to the energy liberation, respectively. Mashima *et al*. [9] have proposed a more detailed muscle model based on the Hill's model in the following way:

$$f_m(\alpha, \dot{l}) = \begin{cases} \frac{bf_0 - a\dot{l}}{|\dot{l}| + b}\alpha & \text{if } \dot{l} \geq 0 \\ \frac{bf_0 - (2f_0 + a)\dot{l}}{|\dot{l}| + b}\alpha & \text{if } \dot{l} < 0 \end{cases} \tag{12}$$

where $0 \leq \alpha \leq 1$ stands for the muscle activation level. The value of the constants a and b have been determined experimentally as $a = 0.25 \cdot |f_0|$, $b = 0.9 \cdot |l_0|$ [9], where l_0 denotes the intrinsic rest length of the muscle. Muscle forces are known to be proportional to the value of the muscle activation level α; f_0 indicates the maximum output force. Therefore in this paper, we assume that the input to the muscle is defined as $\alpha' = f_0 \cdot \alpha$ [N] to set the dimension of the control input as equal to the muscle force. In addition, the muscle has another nonlinear property that can only generate a contractile force. Therefore, the control input to muscles α' should be modified to $\bar{\alpha}$ as a saturated function such that

$$\bar{\alpha} = \begin{cases} 0 & \text{if } \alpha' \leq 0 \\ \alpha' & \text{if } \alpha' > 0 \end{cases}. \tag{13}$$

If the control inputs to the muscles become some negative values, then these values must be re-shaped to zero to satisfy $\bar{\alpha} \geq 0$. By considering these definitions, (12) can be rewritten in the following way:

$$f_m(\bar{\alpha}, \dot{l}) = p\left(\bar{\alpha} - \bar{\alpha}c\dot{l}\right), \tag{14}$$

where

$$p = \frac{0.9l_0}{0.9l_0 + |\dot{l}|},$$
$$c = \begin{cases} \frac{0.25}{0.9l_0} > 0 & \text{if } \dot{l} \geq 0 \\ \frac{2.25}{0.9l_0} > 0 & \text{if } \dot{l} < 0 \end{cases}.$$

In (14), the parameter p which depends on the contractile velocity $\dot{l}$ satisfies $0 < p \leq 1$ as far as $\dot{l}$ is upper-bounded. The system considered here has six muscles, and thereby all the muscle dynamics can be expressed in the following way:

$$\boldsymbol{f}_m = \boldsymbol{P}\bar{\boldsymbol{\alpha}} - \boldsymbol{P}\boldsymbol{A}(\bar{\boldsymbol{\alpha}})\boldsymbol{C}\dot{\boldsymbol{l}}, \tag{15}$$

where

$$\begin{aligned} \boldsymbol{f}_m &= [f_{m_1}, f_{m_2}, \cdots, f_{m_6}]^{\mathrm{T}} \in \mathbb{R}^6 \\ \bar{\boldsymbol{\alpha}} &= [\bar{\alpha}_1, \bar{\alpha}_2, \cdots, \bar{\alpha}_6]^{\mathrm{T}} \in \mathbb{R}^6 \\ \boldsymbol{P} &= \mathrm{diag}[p_1, p_2, \cdots, p_6] \in \mathbb{R}^{6\times 6} \\ \boldsymbol{A}(\bar{\boldsymbol{\alpha}}) &= \mathrm{diag}[\bar{\alpha}_1, \bar{\alpha}_2, \cdots, \bar{\alpha}_6] \in \mathbb{R}^{6\times 6} \\ \boldsymbol{C} &= \mathrm{diag}[c_1, c_2, \cdots, c_6] \in \mathbb{R}^{6\times 6}. \end{aligned}$$

Note that the diagonal matrix $\boldsymbol{A}$ is composed of the elements of the control input vector $\bar{\boldsymbol{\alpha}}$. In fact, $\boldsymbol{A}$ originates from nonlinearity of the muscle model, and it satisfies $\boldsymbol{A} \geq 0$ from (13).

III. ITERATIVE LEARNING CONTROL

A. Desired Trajectory

The purpose of this study is to acquire and evaluate output muscle forces in the case in which a desired end-point trajectory is realized. To do this, we assume that the desired end-point trajectory is given in advance. Especially in this paper, the desired end-point trajectory is given as a line segment in the task space. Its time trajectory is subject to the minimum-jerk criterion, which has been proposed by Flash and Hogan [7]. The performance function to minimize the square of the jerk at the end-point is given as the following way,

$$C = \int_0^T \|\dddot{\boldsymbol{x}}(t)\|^2 \mathrm{d}t, \tag{16}$$

where T is a duration time of the movement, and $\dddot{\boldsymbol{x}}$ stands for a jerk of the end-point in the task-space. By calculating (16), we obtain the specific desired trajectory expressed as follows:

$$\boldsymbol{x}_d(t) = \boldsymbol{x}_0 + (\boldsymbol{x}_f - \boldsymbol{x}_0)\,\omega\left(\tfrac{t}{T}\right), \tag{17}$$

where

$$\omega\left(\tfrac{t}{T}\right) = 6\left(\tfrac{t}{T}\right)^5 - 15\left(\tfrac{t}{T}\right)^4 + 10\left(\tfrac{t}{T}\right)^3.$$

Equation (17) indicates a line segment trajectory designed in the task space. In (17), $\boldsymbol{x}_0$ signifies an initial position of the end-point, $\boldsymbol{x}_f$ denotes a desired final position of that. Note that the optimality of a trajectory of the end-point is not treated in this paper because it is beyond the scope of the paper. As described in the paper, the minimum-jerk criterion is introduced just for the time being. We can easily introduce any other optimal trajectories that have been proposed in physiology or robotics (e.g. Todorov's work [10], etc...) instead of the minimum-jerk criterion.

B. Iterative Learning Control Scheme

In order to realize a given desired trajectory, we employ a PI-type iterative learning control scheme [8]. The construction of the learning control signals has three candidates of learning space: the muscle length space, the joint space, and the task space. As described in this paper, the learning space is chosen as the muscle length space to examine the internal forces generated specifically by the redundant muscles. The

PI-type iterative learning control method in the muscle length space is that the time series error datasets of the muscle's trajectory regarding its length and contractile velocity are stored during one trial. These learning datasets, in which the time series error datasets are multiplied by the learning gains, are added to the control input for the subsequent trial. The control signal for the muscles at the i^{th} trial is given as the following.

$$\bar{\boldsymbol{\alpha}}_i = -\boldsymbol{K}_p \Delta \boldsymbol{l}_i - \boldsymbol{K}_v \Delta \dot{\boldsymbol{l}}_i + \boldsymbol{v}_i, \tag{18}$$

where a subscript i represents the trial number, $\boldsymbol{K}_p = \mathrm{diag}[k_{p_1}, k_{p_2}, \cdots, k_{p_6}] \in \mathbb{R}^{6\times 6} > \boldsymbol{0}$ denotes a feedback gain matrix for the muscle lengths, $\boldsymbol{K}_v = \mathrm{diag}[k_{v_1}, k_{v_1}, \cdots, k_{v_6}] \in \mathbb{R}^{6\times 6} > \boldsymbol{0}$ denotes a feedback gain matrix for the muscle contractile velocities, and $\boldsymbol{v}_i$ is the feed-forward term. The vector $\Delta \boldsymbol{l}_i = \boldsymbol{l}_i - \boldsymbol{l}_d \in \mathbb{R}^6$ signifies the error vector for muscle length and $\Delta \dot{\boldsymbol{l}}_i = \dot{\boldsymbol{l}}_i - \dot{\boldsymbol{l}}_d \in \mathbb{R}^6$ is the error vector for muscle contractile velocity. The desired trajectory is designed in the task space, and thereby these error vectors can be obtained by using (1), (2), (9), and (10). They are given in the following way:

$$\begin{aligned} \Delta \boldsymbol{l} &= \boldsymbol{G}_l(\boldsymbol{q}) - \boldsymbol{G}_l(\boldsymbol{q}_d) \\ &= \boldsymbol{G}_l(\boldsymbol{G}_x^{-1}(\boldsymbol{x})) - \boldsymbol{G}_l(\boldsymbol{G}_x^{-1}(\boldsymbol{x}_d)), \end{aligned} \tag{19}$$

$$\Delta \dot{\boldsymbol{l}} = \boldsymbol{W}^{\mathrm{T}} \Delta \dot{\boldsymbol{q}} = \boldsymbol{W}^{\mathrm{T}} \boldsymbol{J}^{-1} \Delta \dot{\boldsymbol{x}}. \tag{20}$$

The desired muscle length $\boldsymbol{l}_d \in \mathbb{R}^6$ and the muscle contractile velocity $\dot{\boldsymbol{l}}_d \in \mathbb{R}^6$ are given as time-dependent trajectories. The feed-forward term $\boldsymbol{v}_i \in \mathbb{R}^6$ is given by the iterative learning scheme, and it is updated in the following manner:

$$\boldsymbol{v}_i = \begin{cases} \boldsymbol{0} & \text{if } \ i = 1 \\ \boldsymbol{v}_{i-1} - \left(\boldsymbol{\Phi} \Delta \boldsymbol{l}_{i-1} + \boldsymbol{\Psi} \Delta \dot{\boldsymbol{l}}_{i-1} \right) & \text{if } \ i > 1 \end{cases}, \tag{21}$$

where $\boldsymbol{\Phi} = \mathrm{diag}[\phi_1, \phi_1, \cdots, \phi_6] \in \mathbb{R}^{6\times 6} > \boldsymbol{0}$ and $\boldsymbol{\Psi} = \mathrm{diag}[\psi_1, \psi_2, \cdots, \psi_6] \in \mathbb{R}^{6\times 6} > \boldsymbol{0}$ are the position and velocity learning gain matrices, respectively.

C. Dynamics

The dynamics of the two-link planar arm model is known to be expressible in the following way:

$$\boldsymbol{H}(\boldsymbol{q})\ddot{\boldsymbol{q}} + \left\{ \frac{1}{2}\dot{\boldsymbol{H}}(\boldsymbol{q}) + \boldsymbol{S}(\boldsymbol{q}, \dot{\boldsymbol{q}}) \right\} \dot{\boldsymbol{q}} = \boldsymbol{\tau}, \tag{22}$$

where $\boldsymbol{H}(\boldsymbol{q}) \in \mathbb{R}^{2\times 2}$ denotes an inertia matrix, and $\boldsymbol{S}(\boldsymbol{q}, \dot{\boldsymbol{q}}) \in \mathbb{R}^{2\times 2}$ denotes a skew-symmetric matrix which includes Coriolis and centrifugal forces, and $\boldsymbol{\tau} \in \mathbb{R}^2$ is an input torque vector. Substituting (3), (15), and (18) into (22) yields:

$$\begin{aligned} \boldsymbol{H}_i(\boldsymbol{q}_i)\ddot{\boldsymbol{q}}_i + \left\{ \frac{1}{2}\dot{\boldsymbol{H}}_i(\boldsymbol{q}_i) + \boldsymbol{S}_i(\boldsymbol{q}_i, \dot{\boldsymbol{q}}_i) \right\} \dot{\boldsymbol{q}}_i = \\ - \boldsymbol{W}_i \boldsymbol{P}_i \boldsymbol{K}_p \Delta \boldsymbol{l}_i - \boldsymbol{W}_i \boldsymbol{P}_i \boldsymbol{K}_v \Delta \dot{\boldsymbol{l}}_i \\ + \boldsymbol{W}_i \boldsymbol{P}_i \boldsymbol{v}_i - \boldsymbol{W}_i \boldsymbol{P}_i \boldsymbol{A}_i \boldsymbol{C} \boldsymbol{W}_i^{\mathrm{T}} \dot{\boldsymbol{q}}_i. \end{aligned} \tag{23}$$

Equation (23) indicates the dynamics of the overall system in the i^{th} trial, which is expressed in joint space. The first and second terms of the right-hand side of (23) are the muscle length and muscle contractile velocity feedback control signals. The third term is the feed-forward signal generated by the iterative learning control scheme to realize trajectory tracking. Moreover, the fourth term is the damping effect in joint space. It includes the control input matrix $\boldsymbol{A}$. For that reason, it depends on the control signal $\bar{\boldsymbol{\alpha}}$ which includes both feedback and feed-forward control signals.

IV. DYNAMIC DAMPING ELLIPSOID

We assume that the muscular force pattern to realize a given desired trajectory can be acquired by the iterative learning control scheme proposed in the previous section. How is the damping effect at the end-point expressed in the fourth term of the right-hand side of Eq. (23) shaped when the desired trajectory is realized? To evaluate the damping effect of the end-point, we introduce the dynamic damping ellipsoid. The basic idea of the damping ellipsoid at the end-point was proposed by Tsuji *et al.* [11] to measure and evaluate the mechanical impedance of the end-point of a human arm's movement. Specifically, when the end-point of the human's arm in static situation is perturbed by some external forces, a mechanical impedance parameterized by inertia, stiffness, and viscosity coefficients is derived under a linear-approximated human arm's dynamics, and their impedance parameters are expressed as ellipsoids at the end-point. Namely, the damping ellipsoid proposed by Tsuji *et al.* is used from the viewpoint of quasi-static inverse dynamics. In contrast, the objective of introducing the dynamic damping ellipsoid here is to measure and evaluate how the damping ellipsoid generated by the control input is shaped when a given desired end-point trajectory is realized, and how it affects its own movements. In other words, different from Tsuji's motivation to use the damping ellipsoid, that presented here is used from the viewpoint of the control scheme and the forward dynamics. Note again that the dynamic damping ellipsoid is introduced to evaluate the resultant internal forces when the desired trajectory is realized. Figure 3 presents a schematic of the dynamic damping ellipsoid. Next, we specifically examine the part of the control signals expressed as the fourth term of the right-hand-side of (23), which is related only to a joint damping effect. It is given in the following manner:

$$\boldsymbol{\tau}_{\boldsymbol{D}i} = -\boldsymbol{W}_i \boldsymbol{P}_i \boldsymbol{A}_i \boldsymbol{C} \boldsymbol{W}_i^{\mathrm{T}} \dot{\boldsymbol{q}}_i \in \mathbb{R}^2, \tag{24}$$

where $\boldsymbol{\tau}_{\boldsymbol{D}i}$ stands for a damping joint torque generated by internal forces and the control input. The damping term expressed as Eq. (24) includes the control input matrix $\boldsymbol{A}_i$. Thereby the damping effect can be modulated by the control signal $\boldsymbol{A}_i$. On the other hand, an end-point damping force $\boldsymbol{F}_{\boldsymbol{D}i}$ can be expressed as $\boldsymbol{\tau}_{\boldsymbol{D}i}$ as

$$\boldsymbol{F}_{\boldsymbol{D}i} = -\boldsymbol{D}_i \dot{\boldsymbol{x}}_i \in \mathbb{R}^2, \tag{25}$$

where

$$\boldsymbol{D}_i = -\boldsymbol{J}_i^{-\mathrm{T}} \boldsymbol{W}_i \boldsymbol{P}_i \boldsymbol{A}_i \boldsymbol{C} \boldsymbol{W}_i^{\mathrm{T}} \boldsymbol{J}_i^{-1} \in \mathbb{R}^{2\times 2},$$

and $\boldsymbol{J}_i^{-\mathrm{T}} \in \mathbb{R}^{2\times 2}$ indicates the inverse of the transposed Jacobian matrix $\boldsymbol{J}_i^{\mathrm{T}} \in \mathbb{R}^{2\times 2}$. Therefore, the dynamic damping

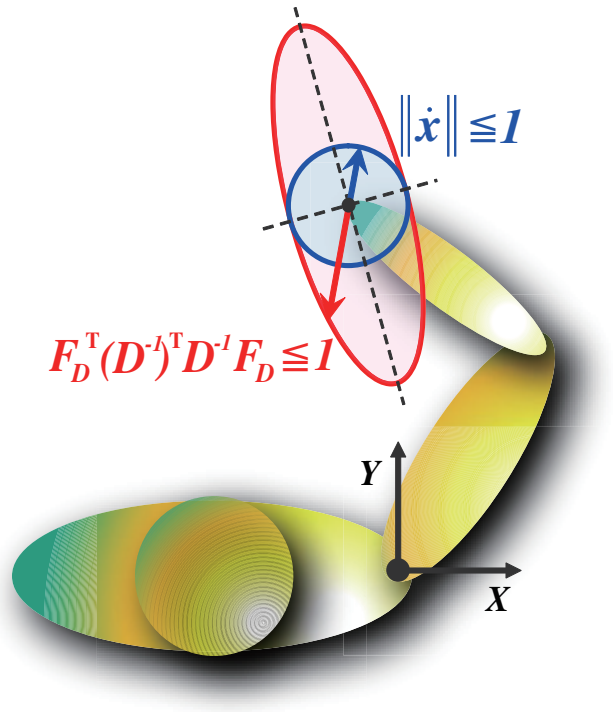

Fig. 2. Dynamic damping ellipsoid at the end-point

ellipsoid at the end-point, which strongly depends on the given control input, is obtainable as long as the end-point velocity satisfies $\|\dot{\boldsymbol{x}}\| \leq 1$ in the following manner:

$$\boldsymbol{F}_{\boldsymbol{D}_i}{}^{\mathrm{T}}(\boldsymbol{D}_i^{-1})^{\mathrm{T}}\boldsymbol{D}_i^{-1}\boldsymbol{F}_{\boldsymbol{D}i} \leq 1. \tag{26}$$

Note that the dynamic damping ellipsoid presented here is composed solely of the control input matrix $\boldsymbol{A}_i$. It does not include the effect of the robot arm dynamics.

It is well-known that the redundant tensile forces generated by some linear actuators, e.g., in a parallel wire-driven system [12], can be basically distributed into two mutually orthogonal spaces. One is composed only of the driving forces to generate the joint torques. The other comprises the internal forces that are not contributed to the arm's movements. However, in our model, the internal forces can affect the arm's movement because of the nonlinearity of the muscles. As shown in the fourth term of the right-hand side of (23), the joint damping effect can be generated not only by the driving forces, but also by the internal forces. The arm's movement is changeable when the internal forces are changed during movement. Therefore, in this paper, the output forces of the muscles are distributed into these two spaces to investigate the effect of the internal forces for the arm's movements. Our proposed iterative learning controller, as presented in Eq. (18) is designed in the muscle length space. Thereby, the input to the muscles $\bar{\boldsymbol{\alpha}}$ is expressible as the summation of the two mutually orthogonal spaces in the following expression:

$$\bar{\boldsymbol{\alpha}}_i = \bar{\boldsymbol{\alpha}}_{drv_i} + \bar{\boldsymbol{\alpha}}_{int_i}, \tag{27}$$

where

$$\bar{\boldsymbol{\alpha}}_{drv_i} = \boldsymbol{W}_i^{+}\boldsymbol{W}_i\bar{\boldsymbol{\alpha}}_i, \quad \bar{\boldsymbol{\alpha}}_{int_i} = \left(\boldsymbol{I}_6 - \boldsymbol{W}_i^{+}\boldsymbol{W}_i\right)\bar{\boldsymbol{\alpha}}_i,$$

and both matrices $\boldsymbol{W}_i^{+}\boldsymbol{W}_i \in \mathbb{R}^{6\times 6}$ and $\left(\boldsymbol{I}_6 - \boldsymbol{W}_i^{+}\boldsymbol{W}_i\right) \in \mathbb{R}^{6\times 6}$ are the projection matrices. They are the mutually orthogonal subspaces, namely, $\bar{\boldsymbol{\alpha}}_{drv_i} \perp \bar{\boldsymbol{\alpha}}_{int_i}$. Therefore, the dynamic damping ellipsoid can also be distributed into two ellipsoids. One is generated by $\bar{\boldsymbol{\alpha}}_{drv_i}$. The other is also generated by $\bar{\boldsymbol{\alpha}}_{int_i}$. These are given as

$$\begin{aligned}&\boldsymbol{F}_{\boldsymbol{D}_i}{}^{\mathrm{T}}(\boldsymbol{D}_i^{-1})^{\mathrm{T}}\boldsymbol{D}_i^{-1}\boldsymbol{F}_{\boldsymbol{D}i} = \\ &\boldsymbol{F}_{\boldsymbol{D}_i}{}^{\mathrm{T}}\left\{(\boldsymbol{D}_{drv_i}^{-1})^{\mathrm{T}}\boldsymbol{D}_{drv_i}^{-1} + (\boldsymbol{D}_{int_i}^{-1})^{\mathrm{T}}\boldsymbol{D}_{int_i}^{-1}\right\}\boldsymbol{F}_{\boldsymbol{D}i} \leq 1,\end{aligned} \tag{28}$$

where

$$\begin{aligned}\boldsymbol{D}_{drv_i} &= -\boldsymbol{J}_i^{-\mathrm{T}}\boldsymbol{W}_i\boldsymbol{P}_i\boldsymbol{A}_{drv_i}\boldsymbol{C}\boldsymbol{W}_i^{\mathrm{T}}\boldsymbol{J}_i^{-1} \in \mathbb{R}^{2\times 2}\\ \boldsymbol{D}_{int_i} &= -\boldsymbol{J}_i^{-\mathrm{T}}\boldsymbol{W}_i\boldsymbol{P}_i\boldsymbol{A}_{int_i}\boldsymbol{C}\boldsymbol{W}_i^{\mathrm{T}}\boldsymbol{J}_i^{-1} \in \mathbb{R}^{2\times 2}\\ \boldsymbol{A}_{drv_i} &= \mathrm{diag}[\bar{\boldsymbol{\alpha}}_{drv_i}] \in \mathbb{R}^{6\times 6}\\ \boldsymbol{A}_{int_i} &= \mathrm{diag}[\bar{\boldsymbol{\alpha}}_{int_i}] \in \mathbb{R}^{6\times 6}.\end{aligned}$$

Therefore, the driving forces and the internal forces generated by the input to the muscles $\bar{\boldsymbol{\alpha}}_i$, which affect the dynamic damping ellipsoid, can be expressed independently as (28). As described in this paper, the internal forces, which can be acquired when the end-point realizes the desired adequate trajectories according to the minimum-jerk criterion, are called one of the "adequate" internal forces.

V. NUMERICAL SIMULATION

In this section, we discuss the shape and its physical meaning of the dynamic damping ellipsoid through numerical simulation results. Tables I to IV show physical parameters, a desired trajectory, and each gain used in the simulation.

Figure 3 shows the dynamic damping ellipsoid when a desired line segment trajectory is realized after the 100$^{\mathrm{th}}$ trial. We see from this figure that the desired line segment trajectory is mostly realized by the iterative learning control scheme expressed as (18) even though the muscle model has strong nonlinearities. Especially, each muscles can only

TABLE I
PHYSICAL PARAMETERS OF THE ARM MODEL

	Length [m]	Mass [kg]	Inertia [kg·m^2]	Mass center [m]
Upper arm	0.31	1.93	0.0141	0.165
Forearm	0.34	1.52	0.0188	0.170

TABLE II
INSERTIONS OF THE MUSCLES

Muscle	Value [m]	
l_1	a_1 = 0.055	b_1 = 0.080
l_2	a_2 = 0.055	b_2 = 0.080
l_3	a_3 = 0.030	b_3 = 0.120
l_4	a_4 = 0.030	b_4 = 0.120
l_5	a_{51} = 0.040	a_{52} = 0.045
l_6	a_{61} = 0.040	a_{62} = 0.045

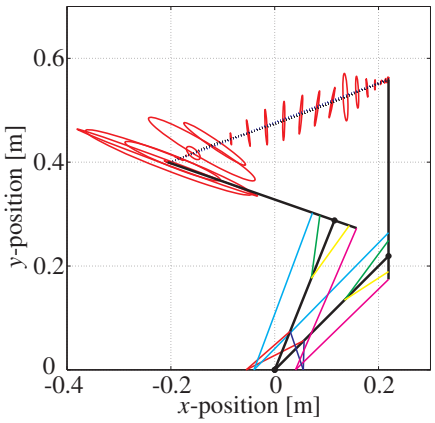

Fig. 3. Dynamic damping ellipsoid which is composed of both "*the internal force*" and "*the driving force*" when the desired linear trajectory is realized after the 100$^{\text{th}}$ trial

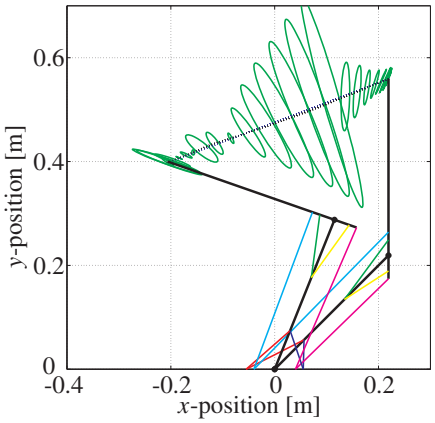

Fig. 4. Dynamic damping ellipsoid which is composed only of "*the internal force*" when the desired linear trajectory is realized after the 100$^{\text{th}}$ trial

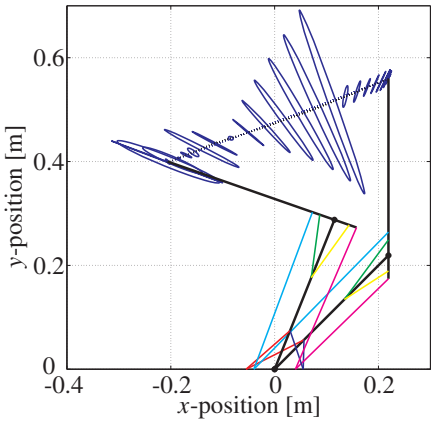

Fig. 5. Dynamic damping ellipsoid which is composed only of "*the driving force*" when the desired linear trajectory is realized after the 100$^{\text{th}}$ trial

TABLE III

DESIRED LINEAR TRAJECTORY

Initial position $\boldsymbol{x}_0$	$[0.22, 0.56]^{\mathrm{T}}$ [m],
Final position $\boldsymbol{x}_f$	$[-0.20, 0.40]^{\mathrm{T}}$ [m],
Duration Time T	0.8 [s]

TABLE IV

FEEDBACK AND LEARNING GAINS

Muscle length feedback gain	$\boldsymbol{K}_p$	$300\boldsymbol{I}_6$
Muscle contractile velocity feedback gain	$\boldsymbol{K}_v$	$200\boldsymbol{I}_6$
Muscle length learning gain	$\boldsymbol{\Phi}$	$90\boldsymbol{I}_6$
Muscle contractile velocity learning gain	$\boldsymbol{\Psi}$	$80\boldsymbol{I}_6$

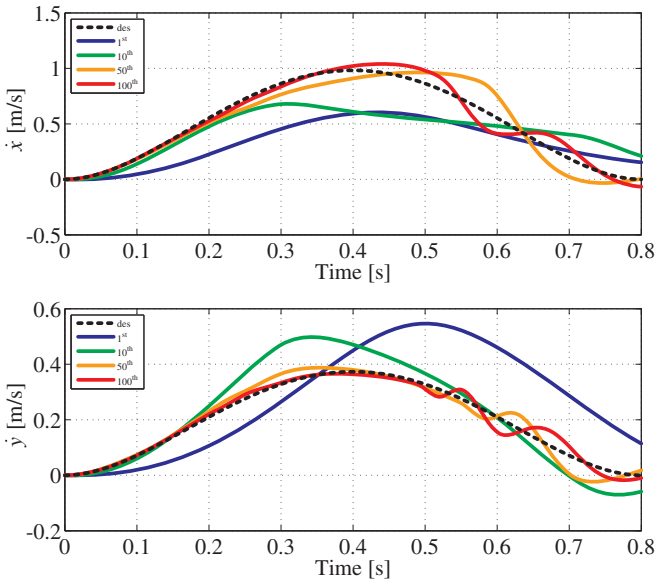

Fig. 6. Transient responses of the end-point velocities after the 1$^{\text{st}}$, 10$^{\text{th}}$, 50$^{\text{th}}$, and the 100$^{\text{th}}$ trial

generate a contractile force, namely, the muscle output force must be larger than 0 [N]. It is quite strong nonlinearity because the output force is discontinuous at 0 [N]. The iterative learning control scheme produces a good performance to track the desired trajectory even though strong nonlinearities exist. Also we can find that the shape of the ellipsoid is drastically changed during movement. It means the internal force is not constant, and it strongly depends on the attitude of the arm and time. Especially in the start phase of the trajectory tracking, the ellipsoid gradually becomes larger, which demonstrates that the end-point position tends to be over the desired trajectory in the start phase. Consequently, the damping effect becomes larger to put the brakes on the end-point movement and thereby inhibit overshooting. As with the start to middle phase, the damping effect becomes much larger to stop the end-point on the desired position in the stop phase. Figures 4 and 5 respectively portray dynamic damping ellipsoids composed solely of the internal forces and driving forces. These figures show that the shapes of both dynamic damping ellipsoids are similar. In addition, both damping ellipsoids are larger than the total dynamic damping ellipsoid, which includes both the feedback control term and the learning control term in the middle phase, indicating that the feedback control term becomes negative; then the damping ellipsoid becomes larger to contain a movement on the end-point. Figure 6 presents velocity profiles of the end-point during trials. As the figure shows, in the start phase, the desired velocity trajectory can be mostly tracked. However, in the stop phase, the velocity profiles tend to be oscillatory, presumably because of the nonlinearity of the muscles. This oscillation can be reduced by repeating trials. Furthermore, the adjustment of the learning gains can reduce it.

Figure 7 depicts the transient responses of the muscular output forces during movement. This figure shows clearly that several terms exist for which each muscle force becomes zero because the control input must satisfy $\bar{\boldsymbol{\alpha}} > 0$, as shown in Eq. (13). Nevertheless, the trajectory tracking is mostly realized, indicating that the learning control scheme is quite effective even under strong nonlinearities. Through the simulation result, we conclude that our proposed iterative learning control scheme can be applicable to the musculoskeletal

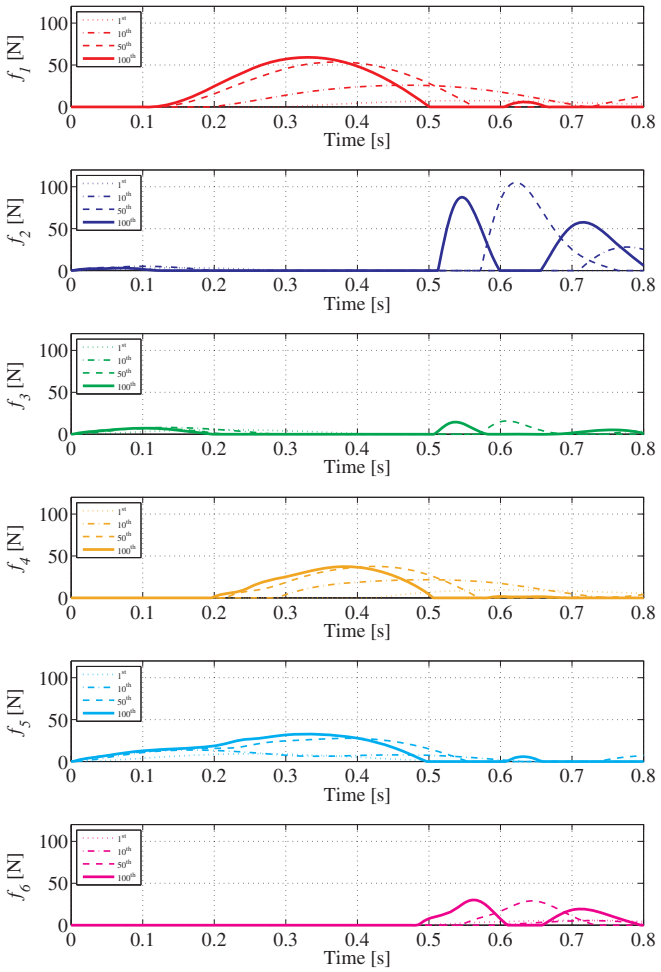

Fig. 7. Transient responses of the muscular forces after the 1st, 10th, 50th, and the 100th trial

redundant system with strong nonlinearities of the muscles.

VI. CONCLUSION

In this paper, we have proposed an iterative learning control method to acquire the given desired trajectories using a musculoskeletal redundant arm model, even under the existence of strong nonlinearities of muscles. Additionally, the dynamic damping ellipsoid has been introduced to evaluate the end-point damping effect acquired through iterative learning. Based on the numerical simulation result, we conclude that the given desired trajectory can be realized through our proposed iterative learning scheme, even under the existence of strong nonlinearities. We also conclude that the value of the internal forces strongly affects the learning speed and its performance. However in this paper, we did not address the strict convergence of the iterative learning control from a theoretical perspective. Moreover, we did not treat joint redundancy. In future works, we must prove the convergence of the iterative learning control scheme under the existence of strong nonlinearities. Furthermore, we will introduce another optimal trajectory criterion to replace the minimum-jerk criterion and provide a comparison of the criteria. In addition, learning spaces can choose not only the muscle length space, as this paper explained, but also the task and the joint space. We will attempt to compare performance and human-similarity with these learning spaces.

ACKNOWLEDGMENT

This work was partially supported by Japan Society for the Promotion of Science (JSPS), Grant-in-Aid for Scientific Research (C) (20560249), and "the Kyushu University Research Superstar Program (SSP)", based on the budget of Kyushu University allocated under President's initiative.

REFERENCES

[1] N. A. Bernstein, "The problem of the interrelation of coordination and localization," *Arch. Biol. Sci.*, Vol. 38, pp. 15–59, 1935.
[2] N. Hogan, "An organizing principle for a class of voluntary movements," *J. Neurosci.*, Vol. 4, No. 11, pp. 2745–2754, 1984.
[3] M. Kawato, K. Furukawa and R. Suzuki, "A hierarchical neural network model for control and learning of voluntary movement," *Biol. Cybern.* Vol. 57, No. 3, 169–185, 1987.
[4] J. Hollerbach and K. Suh, "Redundancy resolution of manipulators through torque optimization," *IEEE Trans. Robot. Autom.*, Vol. 3, No. 4, pp. 308–316, 1987.
[5] S. Arimoto and M. Sekimoto, "Human-like movements of robotic arms with redundant dofs: Virtual spring-damper hypothesis to tackle the Bernstein problem," *Proc. IEEE Int. Conf. Robot. Automat.*, pp. 1860–1866, 2006.
[6] K. Tahara, Z. W. Luo and S. Arimoto, "On control mechanism of human-like reaching movements with musculo-skeletal redundancy," *Proc. IEEE/RSJ Int. Conf. Intell. Robots, Syst.*, pp. 1402–1409, 2006.
[7] T. Flash and N. Hogan, "The coordination of arm movements: An experimentally confirmed mathematical model," *J. Neurosci.*, Vol. 5, No. 7, pp. 1688–1703, 1985.
[8] S. Kawamura, F. Miyazaki and S. Arimoto, "Realization of robot motion based on a learning method," *IEEE Trans. Sys., Man, Cybern.*, Vol. 18, No. 1, pp. 126–134, 1988.
[9] H. Mashima, K. Akazawa, H. Kushima and L. Fujii, "The force-load-velocity relation and the viscous-like force in the frog skeletal muscle," *Jap. J. Physiol.*, Vol. 22, pp. 103–120, 1972.
[10] E. Todorov and M. Jordan, "Optimal feedback control as a theory of motor coordination," *Nature Neuroscience*, Vol. 5, No. 11, pp. 1226–1235, 2002.
[11] T. Tsuji, P. Morasso, K. Goto and K. Ito, "Human hand impedance characteristics during maintained posture," *Biol. Cybern.* Vol. 72, No. 6, pp. 475–485, 1994.
[12] H. Kino, "Principle of orthogonalization for completely restrained parallel wire driven robot," *Proc. IEEE/ASME Int. Conf. Adv. Intell. Mech.*, pp. 509–514, 2003.